arXiv:1407.5356v2 [hep-ph] 1 Aug 2014

Dark Matter Searches in Jet plus Missing Energy in γp collision at CERN LHC

Hao Sun*

Institute of Theoretical Physics, School of Physics & Optoelectronic Technology,

Dalian University of Technology, Dalian 116024, P.R.China

Abstract

In this paper, we investigate the γp photoproduction of jet plus missing energy signal to set limits on the couplings of the fermionic dark matter to the quarks at the LHC via the main reaction pp $\to$ pγp $\to$ p$\chi\chi$j. We assume a typical LHC multipurpose forward detectors and work in a model independent Effective Field Theory framework. Typically, when we do the background analysis, we also include their corresponding Single Diffractive (SD) productions. Our result shows that by requiring a 5σ ($S/\sqrt{B} \geq 5$) signal deviation, with an integrated luminosity of $\mathcal{L} = 200\text{fb}^{-1}$, the lower bounds of WIMP masses scale can be detected up to Λ equal 665.5, 808.9 and 564.0 GeV for the forward detector acceptances ξ_1, ξ_2, and ξ_3, respectively, where $0.0015 < \xi_1 < 0.5$, $0.1 < \xi_2 < 0.5$ and $0.0015 < \xi_3 < 0.15$.

Keywords: Dark Matter, Forward Detector, Large Hadron Collider

PACS numbers: 12.60.-i, 14.70.Bh, 95.35.+d

*haosun@mail.ustc.edu.cn haosun@dlut.edu.cn

1 Introduction

Cosmological observations imply the existence of dark matter (DM) to be the dominant component of cosmical matter[1, 2]. Its relic density has been determined precisely by the WMAP experiment to be $\Omega_\chi h^2 = 0.1109 \pm 0.0056$[3] and it is believed to be non-baryonic, cold, dissipationless and stable on time scales. In addition to these, their physical properties, like making ups or deep natures, are still unknown. Revealing the distribution and the nature of dark matter is one of the most interesting challenges in the fields of both cosmology and particle physics.

Many dark matter candidates have been proposed. Weakly Interacting Massive Particles (WIMPs) is the most compelling one among them. Many beyond the Standard Model (BSM) theories, such as Supersymmetry[4], Warped[5] and Universal[6] Extra Dimensions or Little Higgs Models[7], etc, predict good candidates for the WIMPs and for the cosmological requirements, i.e., the WIMP abundance is a natural consequence of the thermal history of the universe[8]. Although well motivated, there is still no experimental evidence to support these theories. It will be difficult to judge which theory is proper for dark matter. Even the observations of dark matter itself from future experiments may not provide enough information to distinguish underlying theories. In this case, a model independent studies of dark matter phenomenology using Effective Field Theory (EFT) can be particularly important.

Various experiments are set up to hunt for the particle they make up and to reveal the nature of dark matter. For instance, through direct detection (DD) experiments[9, 10, 11, 12], we can search for scattering of dark matter particles from the galactic halo on detector nuclei. Through indirect detection (ID), we can detect dark matter particles by their annihilation into high energy Standard Model (SM) particles [13]. In addition, particle production through high energy accelerators will be another interesting way of dark matter hunting. In this case, the dark matter particles are expected to be detected as a missing component, or manifest as an excess of events showing an imbalance in momentum conservation. There exist some experimental and theoretical studies include,

i.e., the visible radiation of a jet (quark or gluon)[14, 15, 16], a photon[17, 18], or a W/Z boson decaying into leptons or hadronic jets[19, 20, 21] plus the missing "something".

The Large Hadron Collider (LHC) at CERN generates high energetic proton-proton (pp) collisions with a luminosity of $\mathcal{L} = 10^{34}\mathrm{cm}^{-2}\mathrm{s}^{-1}$ and provides the opportunity to study very high energy physics. In such high energy, most attention is usually paid to the central rapidity region where the most of the particles are produced and where the most of the high $\mathrm{p_T}$ signal of new physics is expected. Indeed, the CDF collaboration has already observed such a kind of interesting phenomenon including the exclusive lepton pairs production [22, 23], photon-photon production [24], dijet production [25] and charmonium (J/ψ) meson photoproduction [26], etc. Now, both the ATLAS and the CMS collaborations have programs of forward physics, which are devoted to studies of high rapidity regions, with extra updated detectors located in a place nearly 100-400m close to the interaction point [27, 28]. Technical details of the ATLAS Forward Physics (AFP) projects can be found, for example, in Refs.[29, 30]. The physics program of this new instrumentation covers interesting topics like elastic scattering, diffraction, low-x QCD, Central Exclusive Production (CEP), photon-photon ($\gamma\gamma$) and photo-proton (γp) interactions.

Dark matter searching will be an active topic and an important issue at the LHC[31, 32]. Until now most works are concentrated on its searching through normal pp collision. However, it will also be very interesting to see the status of dark matter searching in photon-photon ($\gamma\gamma$) and photo-proton (γp) interactions. This is mainly due to the reason that photon interactions at the LHC are believed to be simple and clean from challenged backgrounds. The study of photon interactions at the LHC might be a choice of extending the discovery bounds of dark matter as which that will be shown in our discussion. In this paper, we focus on the γp photoproduction of jet plus missing energy signal to set limits on the couplings of the fermionic dark matter to the quarks at the LHC via the main reaction $\mathrm{pp} \to \mathrm{p}\gamma\mathrm{p} \to \mathrm{p}\chi\chi\mathrm{j}$. We assume a typical LHC multipurpose forward detectors and work in a model independent EFT framework. Paper is organized as follow: we build the calculation framework in Section 2 including a brief introduction to γp collision and

to the WIMP production process we are interested in. Section 3 is arranged to present the numerical results and background analysis. Typically, the Single Diffractive (SD) production as background to γp productions is considered. Finally we summarize our conclusions in the last section.

2 Calculation Framework

2.1 γp Collision at the LHC and Equivalent Photon Approximation

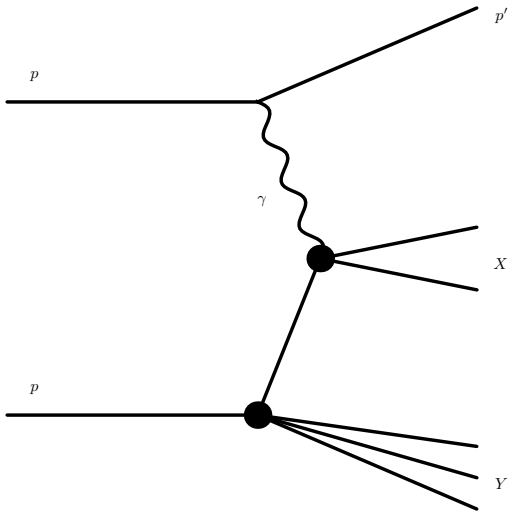

Figure 1: A generic diagram for the photoproduction of pp $\rightarrow$ pγp $\rightarrow$ pXY at the CERN LHC.

Photoproduction is a class of processes in which one of the two interacting protons is not destroyed during the collision but survive into the final state with additional particle (or particles) state(s). Protons of this kind are named intact or forward protons. A generic diagram for the photoproduction denoted as pp $\rightarrow$ pγp $\rightarrow$ pXY is presented in Fig.1. The kinematics of a forward proton is often described by means of the reduced

energy loss ξ, which is also defined as the forward detector acceptance:

$$\xi = \frac{\Delta \mathrm{E}}{\mathrm{E}} = \frac{\mathrm{E} - \mathrm{E}'}{\mathrm{E}} \tag{1}$$

where E is the initial energy of the beam and $\mathrm{s} = 4\mathrm{E}^2$ is the square of the centre of mass energy. E' is the energy after the interaction and ΔE is the energy that the proton lost in the interaction.

The possibility of adding forward proton detectors to both the ATLAS and the CMS experiments has received quite some attention, since the forward proton tagging would provide a very clean environment for new physics searches. Different from usual pp Deep Inelastic Scattering (DIS), incoming protons dissociate into partons, jets will be made from the proton remnants which create some ambiguities and make the new physics signal detection suffer from incredible backgrounds, $\gamma\gamma$ and γp collisions can provide more clean environment. In this case, the quasi-real photons emit with very low virtuality from protons, leave the radiating proton intact, thus provide an extra experimental handle (forward proton tagging) to help reduce the backgrounds. If both incoming and emitted protons remain intact, then it provides the $\gamma\gamma$ collisions, which can be cleaner than the γp collisions. However, γp collisions have higher energy and effective luminosity with respect to $\gamma\gamma$ collisions.

Deflected protons and their energy loss will be detected by the forward detectors with a very large pseudorapidity, while the remaining system will go to central detector. Photons emitted with small angles by the protons show a spectrum of virtuality Q^2 and the energy E_γ. This is described by the Equivalent Photon Approximation (EPA)[33] which differs from the point-like electron (positron) case by taking care of the electromagnetic form factors in the equivalent γ spectrum and effective γ luminosity:

$$\frac{\mathrm{dN}_\gamma}{\mathrm{dE}_\gamma \mathrm{dQ}^2} = \frac{\alpha}{\pi}\frac{1}{\mathrm{E}_\gamma \mathrm{Q}^2}\left[(1 - \frac{\mathrm{E}_\gamma}{\mathrm{E}})(1 - \frac{\mathrm{Q}^2_{\mathrm{min}}}{\mathrm{Q}^2})\mathrm{F}_\mathrm{E} + \frac{\mathrm{E}^2_\gamma}{2\mathrm{E}^2}\mathrm{F}_\mathrm{M}\right] \tag{2}$$

with

$$\mathrm{Q}^2_{\mathrm{min}} = (\frac{\mathrm{M}^2_{\mathrm{inv}}\mathrm{E}}{\mathrm{E} - \mathrm{E}_\gamma} - \mathrm{M}^2_\mathrm{P})\frac{\mathrm{E}_\gamma}{\mathrm{E}}, \quad \mathrm{F}_\mathrm{E} = \frac{4\mathrm{M}^2_\mathrm{p}\mathrm{G}^2_\mathrm{E} + \mathrm{Q}^2\mathrm{G}^2_\mathrm{M}}{4\mathrm{M}^2_\mathrm{p} + \mathrm{Q}^2},$$
$$\mathrm{G}^2_\mathrm{E} = \frac{\mathrm{G}^2_\mathrm{M}}{\mu^2_\mathrm{p}} = (1 + \frac{\mathrm{Q}^2}{\mathrm{Q}^2_0})^{-4}, \quad \mathrm{F}_\mathrm{M} = \mathrm{G}^2_\mathrm{M}, \quad \mathrm{Q}^2_0 = 0.71\mathrm{GeV}^2, \tag{3}$$

where α is the fine-structure constant, E is the energy of the incoming proton beam, which is related to the quasi-real photon energy by $E_\gamma = \xi E$. M_p is the mass of the proton and M_{inv} is the invariant mass of the final state. $\mu_p^2 = 7.78$ is the magnetic moment of the proton. F_E and F_M are functions of the electric and magnetic form factors given in the dipole approximation.

We denote the photoproduction processes in Fig.1 as

$$pp \to p\gamma p \to p + \gamma + q/\bar{q}/g \to p + \underbrace{i + j + k + ...}_{X} + Y \tag{4}$$

with q = u, d, c, s, b and i, j, k, ... the final state particles. The hadronic cross section at the LHC can be converted by integrating $\gamma + q/\bar{q}/g \to i + j + k + ...$ over the photon ($dN(x, Q^2)$), gluon and quark ($G_{g,q/p}(x_2, \mu_f)$) spectra:

$$\sigma_{\gamma p} = \sum_{j=q,\bar{q},g} \int_{\frac{M_{inv}}{\sqrt{s}}}^{\sqrt{\xi_{max}}} 2zdz \int_{Max(z^2,\xi_{min})}^{\xi_{max}} \frac{dx_1}{x_1} \int_{Q^2_{min}}^{Q^2_{max}} \frac{dN_\gamma(x_1)}{dE_\gamma dQ^2} G_{g,q/p}(\frac{z^2}{x_1}, \mu_f) \cdot \int \frac{1}{avgfac} \frac{|\mathcal{M}_n(\gamma j \to klm..., \hat{s} = z^2 s)|^2}{2\hat{s}(2\pi)^{3n-4}} d\Phi_n, \tag{5}$$

where x_1 is the ratio between scattered quasi-real photons and incoming proton energy $x_1 = E_\gamma/E$. $\xi_{min}(\xi_{max})$ are its lower (upper) limits which means the forward detector acceptance satisfies $\xi_{min} \le \xi \le \xi_{max}$. x_2 is the momentum fraction of the proton momentum carried by the gluon (quark). The quantity $\hat{s} = z^2 s$ is the effective center-of-mass system (c.m.s.) energy with $z^2 = x_1 x_2$. $s = 4E^2$ mentioned above and M_{inv} is the total mass of the related final states. $2z/x_1$ is the Jacobian determinant when transform the differentials from $dx_1 dx_2$ into $dx_1 dz$. $G_{g,q/p}(x, \mu_f)$ represent the gluon (quark) parton density functions, μ_f is the factorization scale. $f = \frac{dN}{dE_\gamma dQ^2}$ is the Q^2 dependent relative luminosity spectrum present in Eq.(2). $Q^2_{max} = 2GeV^2$ is the maximum virtuality. $\frac{1}{avgfac}$ is the times of the spin-average factor, the color-average factor and the identical particle factor. $|\mathcal{M}_n|^2$ presents the squared n-particle matrix element and divided by the flux factor $[2\hat{s}(2\pi)^{3n-4}]$. The n-body phase space differential $d\Phi_n$ and its integral Φ_n depend only on $\hat{s}$ and particle

masses m_i due to Lorentz invariance:

$$\begin{aligned}\Phi_n(\hat{s}, m_1, m_2, ..., m_n) &= \int d\Phi_n(\hat{s}, m_1, m_2, ..., m_n) \\ &= \int \delta^4((p_i + p_j) - \sum_{k=1}^{n} p_k) \prod_{k=1}^{n} d^4 p_k \delta(p_k^2 - m_k^2)\Theta(p_k^0) \qquad (6)\end{aligned}$$

with i and j denoting the incident particles and k running over all outgoing particles.

A brief review of experimental prospects for studying photon induced interactions are summarized in Ref.[34]. Many other related phenomenological studies are summarized here: standard model productions[35, 36, 37], supersymmetry[38, 39], extra dimensions[40, 41, 42, 43], unparticle physics[44], top triangle moose model[45], gauge boson self-interactions [46, 47, 48, 49, 50, 51, 52, 53, 54, 55], neutrino electromagnetic properties[56, 57, 58], the top quark physics[59, 60, 61, 36, 37] and triplet Higgs production[62], etc.

2.2 WIMPs production via $pp \to p\gamma p \to p\chi\chi j$

In our study, we assume that the dark matter candidate is the only new particle which is singlet under the SM local symmetries, and all SM particles are singlets under the dark-sector symmetries. The interaction between dark matter and the SM particles are presumably effected by the exchange of some heavy mediators whose nature we do not need to specify, but only assume that they are much heavier than the typical scales. We specialize to the case of a spin-1/2, Dirac fermion and describe the interaction between dark matter and SM quarks accurately in terms of an Effective Field Theory[63]. There consists of the SM Lagrangian plus kinetic terms for the dark matter χ and a set of effective four fermion interactions between χ and the quarks q = u, d, s, c, b, t:

$$\mathcal{L}_{\chi\chi qq} = \sum_q \left[\frac{1}{\Lambda_{D5}^2} \bar{q}\gamma^\mu q \bar{\chi}\gamma_\mu \chi + \frac{1}{\Lambda_{D8}^2} \bar{q}\gamma^\mu\gamma_5 q \bar{\chi}\gamma_\mu\gamma_5 \chi \right] \qquad (7)$$

where χ refers to the dark matter particle. The characterizing parameters Λ_i are the scales of the effective interactions where $\Lambda_i = \frac{M}{\sqrt{g_\chi g_q}}$ with M is the mass of the mediator, g_χ is the coupling to dark matter particle and g_q is its coupling to SM quarks. The first

term in Eq.(7) corresponds to the spin-independent scattering with vector coupling while the second term corresponds to the spin-dependent axial-vector coupling. Here we will consider interactions that yield a spin-independent scattering cross section and simplify our consideration to the vector coupling case. Similarly, our discussion can be easily extended to the other cases.

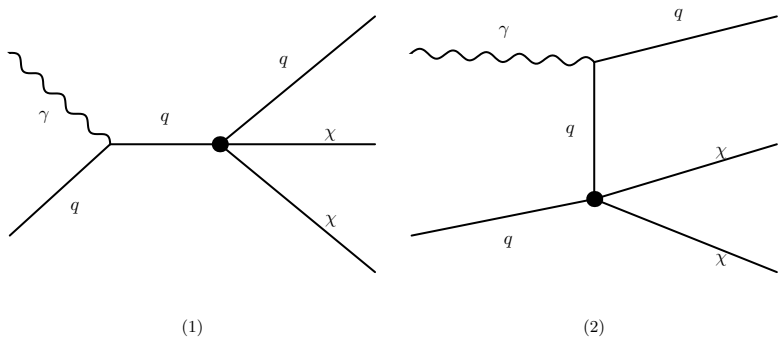

Figure 2: Parton level Feynman diagrams for pp $\to$ pγp $\to$ p$\chi\chi$j include the s-channel contribution (1) and the t-channel contribution (2). Here q=u, d, c, s, b, $\bar{u}$, $\bar{d}$, $\bar{c}$, $\bar{s}$ and $\bar{b}$. Black blobs represent the $\chi\chi$qq couplings parameterized by Eq.(7).

In the effective field theory, WIMP-SM interactions lead to the direct production of WIMPs via the process pp $\to \chi\bar{\chi}$ through the normal pp collision mode at the colliders. In order to contain a visible trace, one can study WIMPs produced together with hard jet(s), γ(s) or heavy gauge boson (W, Z) and provide a trigger within hard scatterings. Different from normal pp collision, no direct production of pp $\to \chi\bar{\chi}$ appear at the γp collider. The simplest production is pp $\to$ pγp $\to$ p + $\chi\bar{\chi}$j. Here jet can not be γ or gluon but only light quarks. The Feynman diagrams can be found in Fig.2. We implement the lagrangian into FeynArts and use the Feynman diagram approach to provide the amplitudes. By inserting the amplitudes into Eq.(5) we can obtain the total photon produced cross section for pp $\to$ pγp $\to$ p$\chi\chi$j at the LHC.

3 Numerical Results

3.1 Input Parameters and Kinematic Cuts

We take the input parameters as $M_p = 0.938272046$ GeV, $\alpha_{ew}(m_Z^2)^{-1}|_{\overline{MS}} = 127.918$, $m_Z = 91.1876$GeV, $m_W = 80.385$ GeV, $\Gamma_W = 2.085$ GeV, $\Gamma_Z = 2.4952$ GeV[64] and we have $\sin^2\theta_W = 1-(m_W/m_Z)^2 = 0.222897$. Light fermion masses are neglected through the whole calculation. The colliding energy in the proton-proton c.m.s. system is assumed to be $\sqrt{s} = 14$ TeV at the future LHC with luminosity taken to be a running parameter. The factorization scale is chosen to be $\mu_f = M_Z$. The strong coupling constant $\alpha_s = 0.118$. We use FeynArts, FormCalc and LoopTools (FFL)[65, 66, 67] packages to generate the amplitudes and perform the numerical calculations for both the signal and the background, with in-house modification that needed. We adopt CT10[68] PDF for the parton distributions during calculation and BASES[69] to do the phase space integration. Based on the forward proton detectors to be installed by the CMS-TOTEM and the ATLAS collaborations we choose the detected acceptances to be

- CMS-TOTEM forward detectors with $0.0015 < \xi_1 < 0.5$
- CMS-TOTEM forward detectors with $0.1 < \xi_2 < 0.5$
- AFP-ATLAS forward detectors with $0.0015 < \xi_3 < 0.15$

which we simply refer to as ξ_1, ξ_2 and ξ_3, respectively. Such forward detected acceptances will force the proton intact together with the p_T cuts of the related proton. In practically the detector (i.e., AFP) is independent of p_T but much sensitive mainly to the ξ value. These acceptances with the following kinematical cuts will implicit the selected events to have an intact proton and to have been tagged by the forward detectors. During calculation we use ξ_1 in default unless otherwise stated. Note that the gap survival probability ($|S|^2$)[70] in forward productions has some process dependence. With early measurements of rapidity gap processes at the LHC, they will provide valuable information on $|S|^2$. We expect that $|S|^2_{\gamma\gamma} > |S|^2_{\gamma p} > |S|^2_{SD}$. In our phenomenon study the survival

probability for γp collision production is chosen to be $|\mathrm{S}|^2_{\gamma\mathrm{p}} = 0.7$, while that for the Single Diffractive (see following) production is chosen to be $|\mathrm{S}|^2_{\mathrm{SD}} = 0.12$.

In all the results present in our work, we impose a cut of pseudorapidity $|\eta| < 2.5$ for the final state particles since central detectors of the ATLAS and CMS have a pseudorapidity $|\eta|$ coverage 2.5. The general acceptance cuts for the events are:

$$\mathrm{p}^{\mathrm{j}}_{\mathrm{T}} \geq 25\mathrm{GeV}, \not{E}^{\mathrm{miss}}_{\mathrm{T}} > 30\mathrm{GeV}, |\eta^{\mathrm{j}}| < 2.5. \tag{8}$$

In order to reduce the backgrounds containing missing energy from processes where, for example, W bosons are produced, we remove such events for which a charged lepton has transverse momenta $\mathrm{p}^{\ell}_{\mathrm{T}} \geq 25\mathrm{GeV}$ and is further separated from all jets by $\Delta\mathrm{R}(\ell\mathrm{j}) > 0.4$[77], where $\Delta\mathrm{R} = \sqrt{\Delta\Phi^2 + \Delta\eta^2}$ is the separation in the rapidity-azimuth plane, $\mathrm{p}^{\mathrm{j},\ell}_{\mathrm{T}}$ are the transverse momentum of jets and leptons and $\not{E}^{\mathrm{miss}}_{\mathrm{T}}$ the missing transverse momentum. We stress here that cuts in Eq.(8) are the basic ones and might change later in our following discussion.

3.2 Background Analysis

As can be seen, the studied topology of our signal therefore give rise to the jet + $\not{E}_{\mathrm{T}}$ signature characterized by one jet and a missing transverse momentum ($\not{E}_{\mathrm{T}}$) from the undetected dark matter pair production. The dominant SM backgrounds consist of the following types:

- γp collision of the SM production of Z+jet where Z decays into a pair of neutrinos:

$$\mathrm{pp} \to \mathrm{p}\gamma\mathrm{p} \to \mathrm{p} + (\mathrm{Z} \to \nu\bar{\nu})\mathrm{j} + \mathrm{Y} \tag{9}$$

- γp collision of the SM W+jet associated production with the W decays into a neutrino and a charged lepton falls outside of the acceptance range of the detector:

$$\mathrm{pp} \to \mathrm{p}\gamma\mathrm{p} \to \mathrm{p} + (\mathrm{W} \to \ell^{\pm}\nu)\mathrm{j} + \mathrm{Y} \tag{10}$$

- Single Diffractive (SD) production of Z+jet as main background to γp collision where Z decays into a pair of neutrinos.

- Single Diffractive (SD) production of W+jet associated production with the W decays into a neutrino and the charged lepton falls outside of the acceptance range of the detector.

The first two in the list belong to the SM electroweak processes with some of their Feynman diagrams presented in Fig.3. The cross section can be obtained by Eq.(5). All the three generations of neutrino $\nu_{e,\mu,\tau}$ are taken into account. The CKM matrix $V_{qq'}$ between different generation of quarks are omitted and assumed to be unit within the same generation.

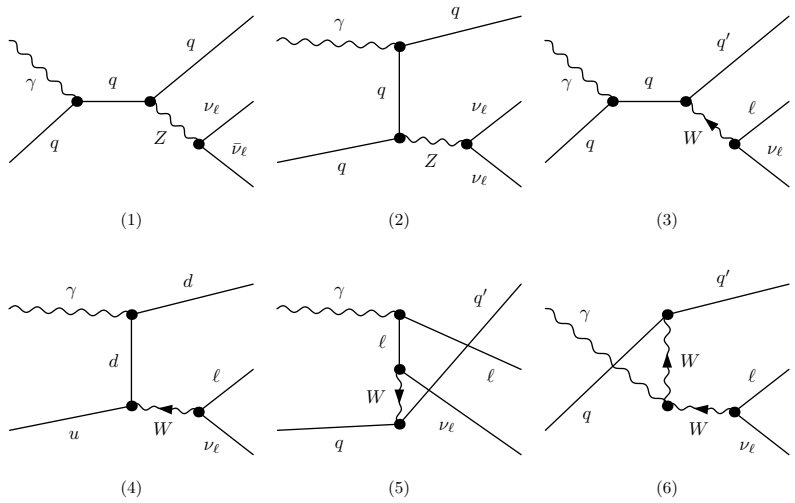

Figure 3: Feynman diagrams for γp collision of the SM production of Z+jet where Z decays into a pair of neutrinos and W+jet associated production with the W decays into a neutrino and a charged lepton falls outside the acceptance range of the detector..

Now lets turn to the last two backgrounds listed ahead whose contributions come from the Single Diffractive productions. SD production is indeed a kind of main background in photoproductions at the γp collider. However, their contributions are usually omitted and not often well considered in some other phenomenological studies. In our paper, we take some efforts to include them and try to find out how important of their contributions will stand in background analysis at the γp collider.

In order to provide a clear image to describe the SD production, in a logical clear way, we start from the description of Double Pomeron Exchange (DPE) production as the main background of $\gamma\gamma$ collision. In DPE, two colorless objects are emitted from both protons. Their partonic components are resolved and create a heavy mass object X ($pp \to p\gamma\gamma p \to pXp$) in the central detector in the Pomeron-Pomeron interaction. The event is characterized by two rapidity gaps between the central object and the protons. Through the exchange of two Pomerons, a dijet system, a diphoton system, a WW and ZZ pair, or a Drell-Yan pair can be created, for instance. The DPE production cross section can be obtained within the factorized Ingelman-Schlein[71] model. In the Ingelman-Schlein model, one assumes that the Pomeron has a well-defined partonic structure, and that the hard process takes place in the Pomeron-proton/proton-Pomeron (single diffraction) or Pomeron-Pomeron (central diffraction) processes. These processes are described in terms of the proton "diffractive" parton distribution functions (DPDFs). Similar to the parton distribution functions, the DPDFs are also obtained from Deep Inelastic Scattering experiments[72, 73]. The difference is that they contain a dependence on some additional variables which are used to describe the proton kinematics: the relative energy loss ξ and four-momentum transfer t, which we introduce as

$$\begin{aligned} g^{D}(x,\mu^2) &= \int dx_{\mathbf{P}} d\beta \delta(x - x_{\mathbf{P}}\beta) g_{\mathbf{P}}(\beta,\mu^2) f_{\mathbf{P}}(x_{\mathbf{P}}) \\ &= \int_{x}^{1} \frac{dx_{\mathbf{P}}}{x_{\mathbf{P}}} f_{\mathbf{P}}(x_{\mathbf{P}}) g_{\mathbf{P}}(\frac{x}{x_{\mathbf{P}}},\mu^2) \end{aligned} \tag{11}$$

where g^{D} denotes either the quark or the gluon distributions with D refers to "diffractive". $f_{\mathbf{P}}(x_{\mathbf{P}})$ is the flux of Pomerons and expressed as

$$f_{\mathbf{P}}(x_{\mathbf{P}}) = \int_{t_{min}}^{t_{max}} f(x_{\mathbf{P}}, t) dt \tag{12}$$

with t_{min} and t_{max} being the kinematic boundaries. $g_{\mathbf{P}}(\beta,\mu^2)$ is the partonic structure of Pomeron. $x_{\mathbf{P}}$ here is the fraction of the proton momentum carried by the Pomeron corresponding to the relative energy loss ξ. And β is the fraction of the Pomeron momentum carried by the struck parton. Both Pomeron flux factors $f(x_{\mathbf{P}}, t)$ as well as quark, gluon distributions in the Pomeron $g_{\mathbf{P}}(\beta,\mu^2)$ were taken from the H1 collaboration analysis

of diffractive structure function at HERA[72, 73]. Therefore, the final forward detector acceptance ξ-dependent convolution integral for the DPE production is given by

$$\sigma_{\rm DPE} = \sum_{\rm ij=q\bar{q},gg,qg,\bar{q}g} \int_{\frac{\rm M_{inv}}{\sqrt{\rm s}}}^{\xi_{\rm max}} 2{\rm zdz} \int_{{\rm Max}(\frac{\rm z^2}{\xi_{\rm max}},\xi_{\rm min})}^{{\rm Min}(\xi_{\rm max},\frac{\rm z^2}{\xi_{\rm min}})} \frac{{\rm dx_1}}{\rm x_1} \int_{\rm x_1}^1 \frac{{\rm dx_{\mathbf{P}_i}}}{\rm x_{\mathbf{P}_i}} {\rm f_{\mathbf{P}_i}(x_{\mathbf{P}_i})} {\rm g_{\mathbf{P}_i}}(\frac{\rm x_1}{\rm x_{\mathbf{P}_i}}, \mu^2)$$
$$\int_{\frac{\rm z^2}{\rm x_1}}^1 \frac{{\rm dx_{\mathbf{P}_j}}}{\rm x_{\mathbf{P}_j}} {\rm f_{\mathbf{P}_j}(x_{\mathbf{P}_j})} {\rm g_{\mathbf{P}_j}}(\frac{\rm z^2}{\rm x_1 x_{\mathbf{P}_j}}, \mu^2) \int \frac{1}{\rm avgfac} \frac{|\mathcal{M}_{\rm n}({\rm ij} \to {\rm klm...}, \hat{\rm s} = {\rm z^2 s})|^2}{2\hat{\rm s}(2\pi)^{3{\rm n}-4}} {\rm d}\Phi_{\rm n}(13)$$

Logically it will now easy to turn to SD production. A Pomeron-proton or proton-Pomeron interaction can be used to describe it and the total SD production cross section can be directly obtained by

$$\sigma_{\rm SD} = \sum_{\rm ij=q\bar{q},gg,qg,\bar{q}g} \int_{\frac{\rm M_{inv}}{\sqrt{\rm s}}}^{\sqrt{\xi_{\rm max}}} 2{\rm zdz} \int_{{\rm Max}({\rm z^2},\xi_{\rm min})}^{\xi_{\rm max}} \frac{{\rm dx_1}}{\rm x_1} \int_{\rm x_1}^1 \frac{{\rm dx_{\mathbf{P}_i}}}{\rm x_{\mathbf{P}_i}} {\rm f_{\mathbf{P}_i}(x_{\mathbf{P}_i})} {\rm g_{\mathbf{P}_i}}(\frac{\rm x_1}{\rm x_{\mathbf{P}_i}}, \mu^2)$$
$${\rm G_{g,q/p}}(\frac{\rm z^2}{\rm x_1}, \mu_{\rm f}) \int \frac{1}{\rm avgfac} \frac{|\mathcal{M}_{\rm n}({\rm ij} \to {\rm klm...}, \hat{\rm s} = {\rm z^2 s})|^2}{2\hat{\rm s}(2\pi)^{3{\rm n}-4}} {\rm d}\Phi_{\rm n}. \qquad (14)$$

Diffraction usually dominates for $\xi < 0.05$ which means we can replace ${\rm Min}(\xi_{\rm max}, \frac{\rm z^2}{\xi_{\rm min}})$ in Eq.(13) or $\xi_{\rm max}$ in Eq.(14) by 0.05 directly. We check this and find the difference is quite small as expected. Due to this reason, we can find that SD background are dominant for $0.0015 < \xi_1 < 0.5$ and $0.0015 < \xi_3 < 0.15$ while strongly suppressed for $0.1 < \xi_2 < 0.5$.

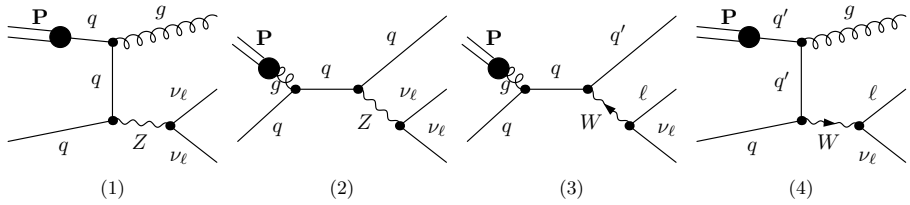

Figure 4: Some Feynman diagrams for Single Diffractive production of Z+jet where Z decays into a pair of neutrinos and W+jet associated production with the W decays into a neutrino and a charged lepton falls outside the acceptance range of the detector.

Feynman diagrams for Single Diffractive production of Z+jet with Z decays into a pair of neutrinos and for that of W+jet associated production with the W decays into a

neutrino and a charged lepton (where the lepton falls outside the acceptance range of the detector), are presented in Fig.4. The double solid lines refer to the Pomeron (**P**) that come from the forward proton and going with a parton (quarks or gluon) emission from inside. The other initial parton comes from the dissociate proton, described in terms of the normal proton PDF. The other diagrams with the inverse of the Pomeron-proton, which means replaced by proton-Pomeron, are similar thus not shown in the figures. Final cross section of the SD productoin can than be obtain by Eq.(14). We add these productions into FormCalc and perform our calculation also with the help of the FFL packages.

3.3 Data and Signal Boundary

In Fig.5 we present the differential cross sections of the transverse momentum of the jet (p_T^{jet}), the invariant mass of the produced System (M_{inv}) and the H_T distributions where $H_T = \sum |p_T^{jet}| + \not{E}_T$. For the signal, we have chosen a WIMP mass of 10 GeV and the effective scale $\Lambda_{D5} = 100$ and 200 GeV. The basic kinematic cuts in Eq.(8) and the survival probability factor $|S|^2{}_{\gamma p} = 0.7$ and $|S|^2{}_{SD} = 0.12$ are taken into account. The forward detector acceptance is chosen to be $0.0015 < \xi_1 < 0.5$. Different sub-contributions of the backgrounds including γp electroweak productions and SD productions are presented. Their total contributions are depicted by the solid lines. Compare these background contributions we can see for $0.0015 < \xi_1 < 0.5$, the dominant background indeed come from SD Z+jet production. The smallest one is the photon produced W+jet production. The γp Z+jet production and SD W+jet production are comparable and not deviate far from each other. No matter which one, all the backgrounds are dominant over the low p_T^{jet} region and reduced rapidly through the high p_T^{jet} region. The same behavior can be found for distributions of M_{inv} and H_T. The dashed and dotted lines present the signal with $\Lambda_{D5} = 100$ GeV and $\Lambda_{D5} = 200$ GeV, respectively. All the p_T^{jet}, M_{inv} and H_T distributions are enhanced by the dark matter effects at larger or higher regions. This potential of distributions clearly provide very simple and effective way to separate the signal from the backgrounds. This is easily and primarily realized by adopting large p_T^{jet} cuts. Just to

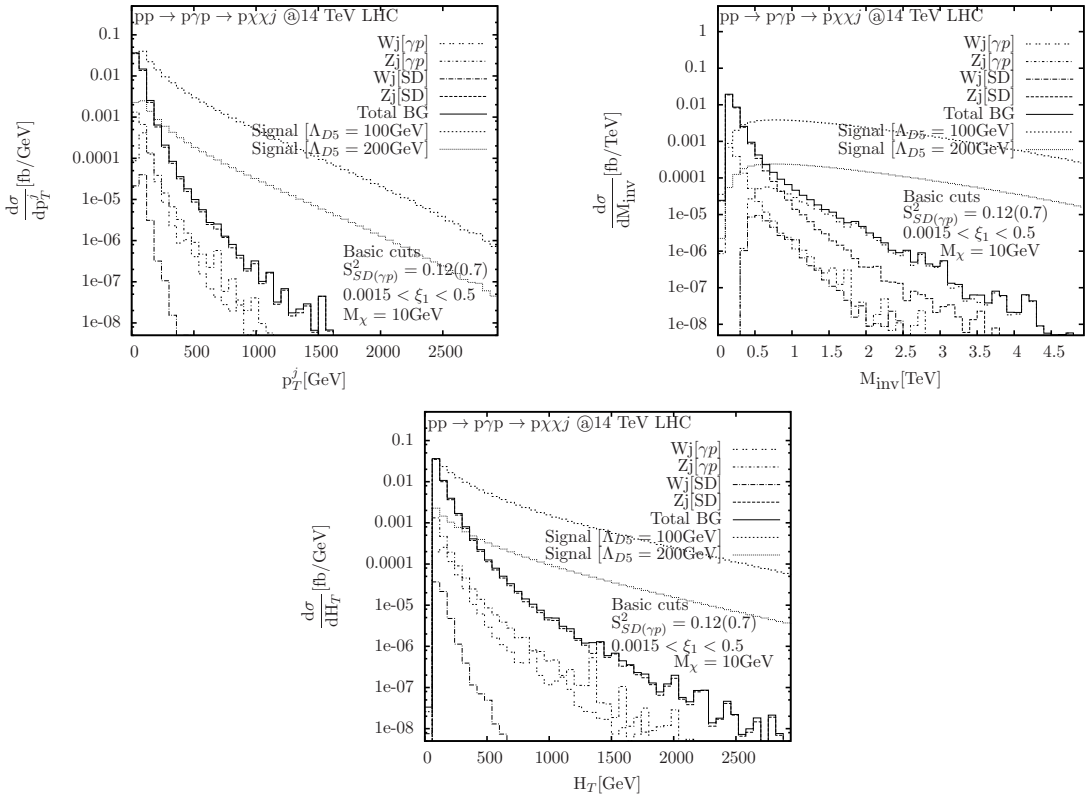

Figure 5: The signal and background differential cross sections of the transverse momentum of the jet (p_T^{jet}), the invariant mass of the produced System (M_{inv}) and the H_T distributions for pp $\rightarrow$ pγp $\rightarrow$ p$\chi\chi$j. The Basic kinematic cuts and survival probability factor are taken into account. The forward detector acceptance is chosen to be $0.0015 < \xi_1 < 0.5$. Here $M_\chi = 10$GeV and $\Lambda_{D5} = 100$ and 200 GeV.

remind here that in Fig.5 we choose the basic kinematic cuts where $p_T^{jet} > 25$ GeV.

In order to see how the cross sections for signal and background depend on the final transverse momentum jet (p_T^{jet}) cuts, we present this dependence in Tab.1 with typical cuts of $p_T^{jet} > 25$ GeV, $p_T^{jet} > 200$ GeV, $p_T^{jet} > 350$ GeV and $p_T^{jet} > 500$ GeV, respectively. We can see that larger p_T^{jet} cut can reduce the background cross section essentially while make the signal reduce slightly. As can be found that the larger p_T^{jet} cut can improve the quantity of the signal over background ratio (S/B), which implies a result that is more robust against systematic uncertainties. We also calculate the statistical significance (SS) for the signal and background on different values of p_T^{jet} cuts in the same table for $\Lambda_{D5} = 300$ GeV with the following formula[74]:

$$SS = \sqrt{2[(S+B)\log(1+\frac{S}{B}) - S]} \tag{15}$$

where S and B are the numbers of signal and background events, respectively. $\mathcal{L}$ presents the luminosity of future 14 TeV LHC where we take the value of 5 and 20 fb^{-1}. We can see the statistical significance of the dark matter effect is large and might be detected. In the following calculation, we apply $p_T^{jet} > 350$ GeV for $0.0015 < \xi_1 < 0.5$. The same table but different values is presented for $0.1 < \xi_1 < 0.5$ in Tab.2. In this case, we apply $p_T^{jet} > 200$ GeV. From our former studies[60] we know that the production behavior for $0.0015 < \xi_1 < 0.15$ is very close to that of $0.0015 < \xi_1 < 0.5$. This has also been calculated and confirmed. Results are not shown here to avoid duplicate. Similarly here we adopt $p_T^{jet} > 350$ GeV.

In Fig.6, we present the signal cross sections of $pp \to p\gamma p \to p\chi\chi j$ as functions of the dark matter scale Λ_{D5} and three forward detector acceptance: $0.0015 < \xi_1 < 0.5$, $0.1 < \xi_2 < 0.5$ and $0.0015 < \xi_3 < 0.15$. Solid, dashed and dotted lines correspond to ξ_1, ξ_2 and ξ_3, respectively. Their cross sections dropped rapidly as Λ_{D5} become larger. For results of Λ_{D5} and Λ_{D8}, their contributions are indeed very close to each other. That's why we only focus our study on Λ_{D5}. Compare different acceptance regions, though they have almost the same features, ξ_1 and ξ_3 do not differ much from each other while both of them are much larger than cross section of ξ_2. Just to remind that here we

σ and SS dependence on p_T^{jet} for $0.0015 < \xi_1 < 0.5$				
σ[pb]	$p_T^j > 25$GeV	$p_T^j > 200$GeV	$p_T^j > 350$GeV	$p_T^j > 500$GeV
σ_{BG}	3.2725	4.0933×10^{-2}	5.1713×10^{-3}	1.1613×10^{-3}
$\sigma_{\Lambda_{D5}=100}$	9.1687	2.9393	1.4921	8.3580×10^{-1}
$\sigma_{\Lambda_{D5}=300}$	1.1323×10^{-1}	3.6288×10^{-2}	1.8421×10^{-2}	1.0318×10^{-2}
$SS^{\mathcal{L}=5}_{\Lambda_{D5}=300}$	4.40079	11.2813	13.1863	12.6422
$SS^{\mathcal{L}=20}_{\Lambda_{D5}=300}$	8.80158	22.5625	26.3726	25.2844

Table 1: The dependence of total signal[$\Lambda_{D5} = 100$ GeV and 300 GeV], background cross sections and statistical significance [$\Lambda_{D5} = 300$ GeV] for $pp \to p\gamma p \to p\chi\chi j$ on typical values of p_T^{jet} cuts. Here $M_\chi = 10$ GeV and unit of the cross section is in pb. The other kinematic cuts and survival probability factor are taken into account. Forward detector acceptance is chosen to be $0.0015 < \xi_1 < 0.5$.

σ and SS dependence on p_T^{jet} for $0.1 < \xi_2 < 0.5$				
σ[pb]	$p_T^j > 25$GeV	$p_T^j > 200$GeV	$p_T^j > 350$GeV	$p_T^j > 500$GeV
σ_{BG}	2.8022×10^{-2}	1.6099×10^{-3}	2.4527×10^{-4}	7.2497×10^{-5}
$\sigma_{\Lambda_{D5}=100}$	4.3063	1.9020	1.1068	6.8305×10^{-1}
$\sigma_{\Lambda_{D5}=300}$	5.3164×10^{-2}	2.3481×10^{-2}	1.3664×10^{-2}	8.4327×10^{-3}
$SS^{\mathcal{L}=5}_{\Lambda_{D5}=300}$	18.2204	21.3139	20.6161	17.9147
$SS^{\mathcal{L}=20}_{\Lambda_{D5}=300}$	36.4408	42.6277	41.2322	35.8294

Table 2: The dependence of total signal[$\Lambda_{D5} = 100$ GeV and 300 GeV], background cross sections and Statistical significance [$\Lambda_{D5} = 300$ GeV] for $pp \to p\gamma p \to p\chi\chi j$ on typical values of p_T^{jet} cuts. Here $M_\chi = 10$ GeV and unit of the cross section is in pb. The other kinematic cuts and survival probability factor are taken into account. Forward detector acceptance is chosen to be $0.1 < \xi_1 < 0.5$.

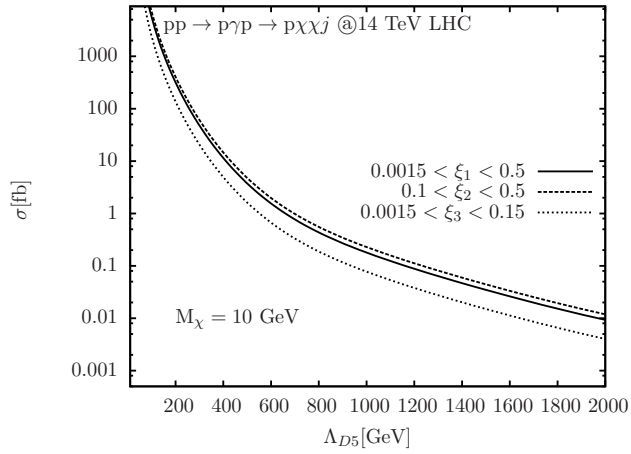

Figure 6: The total cross sections of signal process pp $\to$ pγp $\to$ p$\chi\chi$j as functions of the dark matter effective scale $\Lambda_{\rm D5}$ and three forward detector acceptance regions: $0.0015 < \xi_1 < 0.5$, $0.1 < \xi_2 < 0.5$ and $0.0015 < \xi_3 < 0.15$. Notice here we choose $\rm p_T^{jet} > 350, 200, 300$ GeV for ξ_1, ξ_2 and ξ_3, respectively. The dark matter particle mass is $\rm M_\chi = 10$ GeV.

choose $\rm p_T^{jet} > 350, 200, 350$ GeV for ξ_1, ξ_2 and ξ_3, respectively. That's why cross section of ξ_1 is smaller than that of ξ_2, otherwise if with the same value of $\rm p_T^{jet}$ it will inverse. The SM backgrounds for the main reactions are $\sigma_B = 5.1713$ fb for $0.0015 < \xi_1 < 0.5$, $\sigma_B = 1.6099$ fb for $0.1 < \xi_2 < 0.5$ and $\sigma_B = 3.8062$ fb for $0.0015 < \xi_3 < 0.15$. These numbers will be used in our following data analysis. From this point, we see deviation of the dark matter production from the backgrounds are obvious which might detectable from future experiments.

Now we turn to analyze the potential of the γp collision at the high energy LHC to probe the dark matter signal through photoproduction of $\chi\chi+$jet. We define the 3σ (5σ) discovery significance as

$$\frac{|\sigma_{\rm S+B} - \sigma_{\rm B}|}{\sqrt{\sigma_{\rm B}}}\sqrt{\mathcal{L}} > 3(5) \tag{16}$$

where $\mathcal{L}$ is the integrated luminosity of the γp option of the LHC. In the $\mathcal{L}-\Lambda_{\rm D5}$ parameter space, we present the plots for the 3σ and 5σ deviations of the signal from the total backgrounds. We display our results for the forward detector acceptance chosen to be

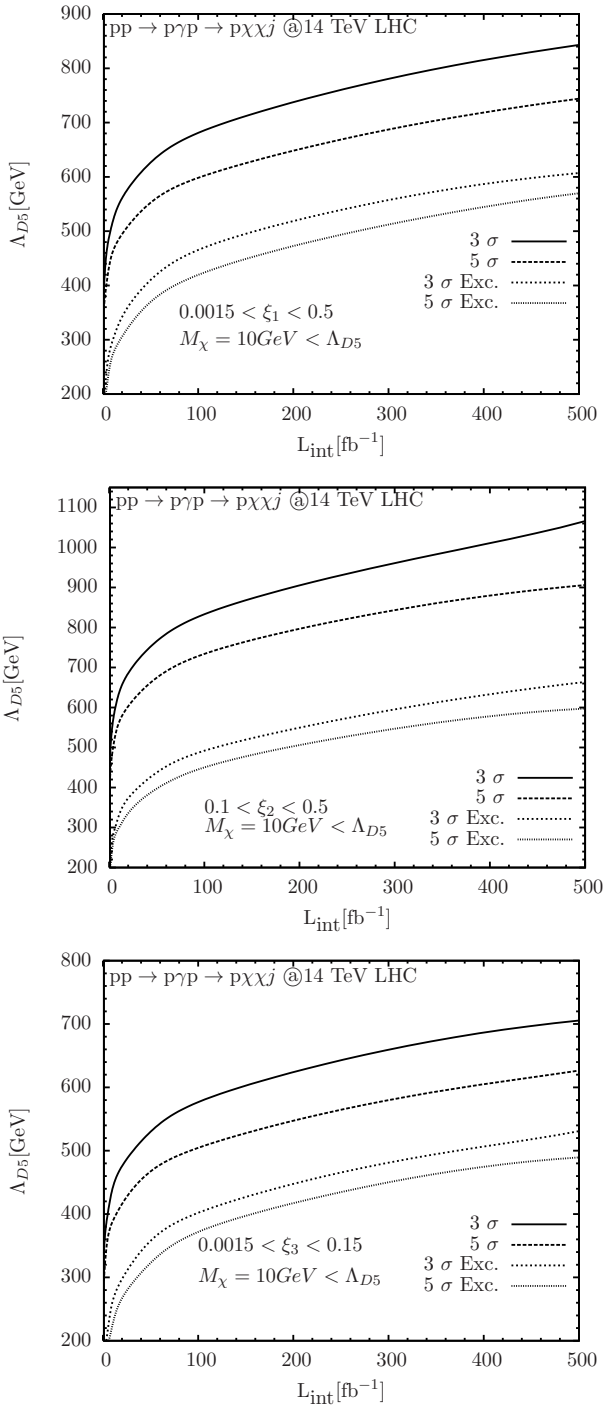

Figure 7: 3σ and 5σ bounds for the dark matter effective scale in the $\mathcal{L} - \Lambda_{\rm D5}$ parameter space, and 3σ and 5σ limit of exclusive boundary where effective field theory may not valid. The dark matter particle mass is $\rm M_\chi = 10$ GeV.

$0.0015 < \xi_1 < 0.5$, $0.1 < \xi_2 < 0.5$ and $0.0015 < \xi_3 < 0.15$ in Fig.7, the first, the second and the third panel, respectively. The center of mass energies of the LHC collider is $\sqrt{s} =$ 14 TeV. Concerning the criteria 5σ deviation of signal from background, with an integrated luminosity $\mathcal{L} = 100\text{fb}^{-1}$, $\text{pp} \to \text{p}\gamma\text{p} \to \text{p}\chi\chi\text{j}$ production through jet photoproduction can probe the dark matter effects up to Λ_{D5} equal 602.7, 748.1 and 510.2 GeV for ξ_1, ξ_2 and ξ_3. With an integrated luminosity $\mathcal{L} = 200\text{fb}^{-1}$ one can probe the dark matter effects up to the mass scale Λ_{D5} equal 665.5, 808.9, 564.0 GeV for ξ_1, ξ_2 and ξ_3, respectively. Here we choose $\text{M}_\chi = 10$ GeV, much less than the scale Λ. We use solid and dashed lines to present the 3σ and 5σ boundary, respectively. Compare these three forward detector acceptances ξ_2 is the most efficient one to detect the dark matter effects. This is mainly because $\xi > 0.5$ belong to the region where single diffractive productions are strongly suppressed, leaving electroweak photoproductions the main background which are indeed quite small with our kinematic cuts, thus lead to a better signal over background ratio. Assuming a 3σ deviation of signal from background, for ξ_2, γp collision of $\chi\chi + \text{jet}$ can probe Λ up to $\sim$ 1TeV, a factor of 2.5 above the best current bounds from LEP-2[75]. Our bounds are comparable with the phenomenological study at a 250 GeV ILC, however, worse than the polarized beams case[76]. Similar studies at the normal pp collider can be found, i.e., in Ref.[77] where the boundary of dark matter mass scale can be probe up to 450 GeV at 14 TeV LHC with the a luminosity of 200 fb^{-1}. Further more, CMS and ATLAS have both carried out the cut-and-count based monojet[15, 16] and monophoton[17, 18] analyses (using $\sim 5\text{fb}^{-1}$ of data). Typically, for the searches through monophoton channel, in the case of D5 spin-independent operator, values of scale below 585 GeV and 156 GeV are excluded at 90% C.L. for M_χ equal to 1 GeV and 1.3 TeV, respectively. Our results show that with the same value of luminosity, the bound obtained is comparable with that obtained by the forward detector acceptance ξ_1, ξ_3, while smaller than that obtained by ξ_2. It should be noted that the contact operator approximation may not be valid if the energy scale of the operator is smaller than the energy scale of the collider process. The bounds we have already obtained may only be somewhat heuristic[78]. This means that an experiment can exclude such a range of $1/\hat{s} > 1/\Lambda^2$. In our case the limit is relevant

for collider dark matter searches, thus $\sqrt{\hat{s}}$ here is the invariant mass of the invisibles. In Fig.7 we also present the 3σ and 5σ limit boundary (with dotted and short dashed curves, respectively) of the range that should be excluded where the effective field theory may not valid.

In Fig.7, we also present the bounds obtained when the luminosity becomes larger than 200fb^{-1}, see, up to 500fb^{-1}. However, we should mention here that as the luminosity become larger, identify the signal under the high pileup running conditions will be challenge: the hadronic background of multiple p-p interactions will be so large that any γp process will be completely swamped. This can be a drawback of γp productions. Even though, purpose of our study does not mean to argue that γp production are better or not to probe dark matter than the other colliders. Instead, the main purpose is to show the potential of γp productions on the dark matter searching. By applying the dark matter searching on the γp production with forward proton tagging we can have at least a general image of the dark matter searching through γp collision after the running of LHC but before the building of future e^-e^+ colliders.

Moreover, the production channel we consider here ($\gamma q \to \chi\chi j$) is related by crossing symmetry to the hard process considered in monophoton dark matter searches ($q\bar{q} \to \chi\chi\gamma$). The advantage of $\gamma q \to \chi\chi j$ production is the reduction in background associated with tagging the intact proton. While the advantage of the monophoton production would be that: a photon in the final state may be cleaner than a jet, and one is more likely to get a $q/\bar{q}$ from the initial proton than a photon. It will also be interesting to study a monophoton search in which the initial q or $\bar{q}$ arises from pomerons which would have a potentially larger production cross-section, and a cleaner final state. A similar study has been presented in Ref.[79] where they concentrate on the Standard Model Z boson production. It can also be extended to the study of new physics, i.e., dark matter searches. A detailed discussion on kinds of these productions might be beyond the scope of this work, we address here the possibility and interesting to study them, and will work on this in a parallel paper.

4 Summary

Dark matter searches at the high energy colliders have received a lot of attention. The study of WIMPs in a model independent Effective Field Theory (EFT) approach is of particularly interesting. Even if a process can be traced back to a definite set of operators, it is rarely the case that a particular collider signature can be traced back to a unique process. For this reason many different, complementary measurements on different collider modes and production channels are usually required to uncover the underlying new physics. LHC provides opportunities to open new fields of the study on the $\gamma\gamma$ and γp collisions with very high energy but very low backgrounds thanks to the forward proton projects. Attention can be paid now to physics in the central rapidity region where the most of the high p_T signal of new physics is expected.

In this paper, we investigate the γp photoproduction of jet plus missing energy signal to set limits on the couplings of the fermionic dark matter to the quarks at the LHC via the main reaction $pp \to p\gamma p \to p\chi\chi j$. We assume a typical LHC multipurpose forward detectors and work in a model independent EFT framework. Typically, when we do the background analysis, we also include their corresponding Single Diffractive (SD) productions. Our result shows that by requiring a 5σ ($S/\sqrt{B} \geq 5$) signal deviation, with an integrated luminosity of $\mathcal{L} = 200 fb^{-1}$, the lower bounds of the dark matter mass scale can be probed up to Λ_{D5} equal 665.5, 808.9, 564.0 GeV for the forward detector acceptances $\xi_1(\xi_2, \xi_3)$, respectively, where $0.0015 < \xi_1 < 0.5$, $0.1 < \xi_2 < 0.5$ and $0.0015 < \xi_3 < 0.15$. Assuming a 3σ deviation of signal from background, for ξ_2, γp collision of $\chi\chi + \text{jet}$ can probe Λ up to $\sim$ 1TeV, a factor of 2.5 above the best current bounds from LEP-2 can comparable with similar studies at the normal pp colliders. By applying the dark matter searching on the γp production with forward proton tagging we present a general image of the dark matter searching at the γp collision after the running of LHC but before the building of future e^-e^+ colliders.

Acknowledgments

The author thanks Fawzi Boudjema for his kindness to provide invaluable comments, thanks Mao Song for useful discussions. Project supported by the National Natural Science Foundation of China (No. 11205070), Shandong Province Natural Science Foundation (No. ZR2012AQ017) and by the Fundamental Research Funds for the Central Universities (No. DUT13RC(3)30).

References

[1] G. Bertone, D. Hooper and J. Silk, *Particle dark matter: Evidence, candidates and constraints*, Phys. Rept. 405 (2005) 279, [arxiv:hep-ph/0404175].

[2] G. Jungman, M. Kamionkowski, K. Griest, *Supersymmetric dark matter*, Phys. Rept. 267 (1996) 195-373, [arxiv:hep-ph/9506380].

[3] E. Komatsu, et al., *Seven-Year Wilkinson Microwave Anisotropy Probe (WMAP) Observations: Cosmological Interpretation*, Astrophys. J. Suppl. 192 (2011) 18, [arXiv:1001.4538].

[4] H. Goldberg, Phys. Rev. Lett. 50 (1983) 1419; J. R. Ellis, J. S. Hagelin, D. V. Nanopoulos, K. A. Olive and M. Srednicki, Nucl. Phys. B 238 (1984) 453; G. L. Kane, C. F. Kolda, L. Roszkowski and J. D. Wells, *Study of Constrained Minimal Supersymmetry*, Phys. Rev. D 49 (1994) 6173-6210 [arXiv:hep-ph/9312272].

[5] K. Agashe and G. Servant, *Warped Unification, Proton Stability and Dark Matter*, Phys. Rev. Lett. 93 (2004) 231805, [arXiv:hep-ph/0403143]; *Baryon Number in Warped GUTs : Model Building and (Dark Matter Related) Phenomenology*, JCAP 0502 (2005) 002, [arXiv:hep-ph/0411254]; K. Agashe, A. Falkowski, I. Low and G. Servant, *KK Parity in Warped Extra Dimension*, JHEP 0804 (2008) 027,

[arXiv:0712.2455]; G. Panico, E. Ponton, J. Santiago and M. Serone, *Dark Matter and Electroweak Symmetry Breaking in Models with Warped Extra Dimensions*, Phys. Rev. D 77 (2008) 115012, [arXiv:0801.1645].

[6] T. Appelquist, H. C. Cheng and B. A. Dobrescu, *Bounds on Universal Extra Dimensions*, Phys. Rev. D 64 (2001) 035002, [arXiv:hep-ph/0012100]; G. Servant and T. M. P. Tait, *Is the Lightest Kaluza-Klein Particle a Viable Dark Matter Candidate?*, Nucl. Phys. B 650 (2003) 391, [arXiv:hep-ph/0206071]; H. C. Cheng, J. L. Feng and K. T. Matchev, *Kaluza-Klein Dark Matter*, Phys. Rev. Lett. 89 (2002) 211301, [arXiv:hep-ph/0207125]; D. Hooper and S. Profumo, *Dark Matter and Collider Phenomenology of Universal Extra Dimensions*, Phys. Rept. 453 (2007) 29-115, [arXiv:hep-ph/0701197]; B. A. Dobrescu, D. Hooper, K. Kong and R. Mahbubani, *Spinless photon dark matter from two universal extra dimensions*, JCAP 0710 (2007) 012, [arXiv:0706.3409].

[7] N. Arkani-Hamed, A. G. Cohen and H. Georgi, *Electroweak symmetry breaking from dimensional deconstruction*, Phys. Lett. B 513 (2001) 232-240, [arXiv:hep-ph/0105239]; H. C. Cheng and I. Low, *TeV Symmetry and the Little Hierarchy Problem*, JHEP 0309 (2003) 051, [arXiv:hep-ph/0308199]; A. Birkedal, A. Noble, M. Perelstein and A. Spray, *Little Higgs Dark Matter*, Phys. Rev. D 74 (2006) 035002, [arXiv:hep-ph/0603077].

[8] J.-L. Feng and J. Kumar, *The WIMPless Miracle: Dark-Matter Particles without Weak-Scale Masses or Weak Interactions*, Phys. Rev. Lett. 101 (2008) 231301, [arXiv:0803.4196]; J.-L. Feng, H. Tu and H.-B. Yu, *Thermal Relics in Hidden Sectors*, JCAP 0810 (2008) 043, [arXiv:0808.2318].

[9] Z. Ahmed, et al., (CDMS and EDELWEISS Collaborations), *Combined Limits on WIMPs from the CDMS and EDELWEISS Experiments*, Phys. Rev. D 84 (2011) 011102, [arXiv:1105.3377].

[10] D. S. Akerib, et al., (LUX Collaboration), *First results from the LUX dark matter experiment at the Sanford Underground Research Facility*, Phys. Rev. Lett. 112 (2014) 091303, [arXiv:1310.8214]; E. Aprile, et al., (XENON100 Collaboration), *Dark Matter Results from 225 Live Days of XENON100 Data*, Phys. Rev. Lett. 109 (2012) 181301, [arXiv:1207.5988].

[11] M. Felizardo, T. A. Girard, T. Morlat, A. C. Fernandes, A. R. Ramos, J. G. Marques, A. Kling and J. Puibasset, et al., *Final Analysis and Results of the Phase II SIMPLE Dark Matter Search*, Phys. Rev. Lett. 108 (2012) 201302, [arXiv:1106.3014]; E. Vazquez-Jauregui, (COUPP Collaboration), *COUPP:Bubble chambers for Dark Matter detection*, in Proceedings of the 48th Rencontres de Moriond on Very High Energy Phenomena in the Universe.

[12] V. Zacek, S. Archambault, E. Behnke, J. Behnke, M. Das, A. Davour, F. Debris and N. Dhungana, et al., *Dark matter search with PICASSO*, J. Phys. Conf. Ser. 375 (2012) 012023.

[13] N.Baro, F.Boudjema, G.Chalons, Sun Hao, *Relic density at one-loop with gauge boson pair production*, Phys. Rev. D 81 (2010) 015005, [arXiv:0910.3293].

[14] CDF Collaboration, *A Search for dark matter in events with one jet and missing transverse energy in $p\bar{p}$ collisions at $\sqrt{s}$ = 1.96 TeV*, Phys. Rev. Lett 108 (2012) 211804, [arXiv:1203.0742].

[15] G. Aad, et al., (ATLAS Collaboration), *Search for dark matter candidates and large extra dimensions in events with a jet and missing transverse momentum with the ATLAS detector*, JHEP 1304 (2013) 075, [arXiv:1210.4491].

[16] S. Chatrchyan, et al., (CMS Collaboration), *Search for dark matter and large extra dimensions in monojet events in pp collisions at $\sqrt{s}$= 7 TeV*, JHEP 1209 (2012) 094, [arXiv:1206.5663].

[17] G. Aad, et al., (ATLAS Collaboration), *Search for dark matter candidates and large extra dimensions in events with a photon and missing transverse momentum in pp collision data at $\sqrt{s}$ = 7 TeV with the ATLAS detector*, Phys. Rev. Lett 110 (2013) 011802, [arXiv:1209.4625].

[18] S. Chatrchyan, et al., (CMS Collaboration), *Search for Dark Matter and Large Extra Dimensions in pp Collisions Yielding a Photon and Missing Transverse Energy*, Phys. Rev. Lett. 108 (2012) 261803, [arXiv:1204.0821].

[19] The ATLAS collaboration, *Search for dark matter pair production in events with a hadronically decaying W or Z boson and missing transverse momentum in pp collision data at $\sqrt{s}$ = 8 TeV with the ATLAS detector*, ATLAS-CONF-2013-073.

[20] CMS Collaboration, (CMS Collaboration), *Search for dark matter in the mono-lepton channel with pp collision events at center-of-mass energy of 8 TeV*, CMS-PAS-EXO-13-004.

[21] G. Aad, et al., (ATLAS Collaboration), *Search for dark matter in events with a hadronically decaying W or Z boson and missing transverse momentum in pp collisions at $\sqrt{s}$=8 TeV with the ATLAS detector*, Phys. Rev. Lett. 112 (2014) 041802, [arXiv:1309.4017].

[22] A. Abulencia, et al., (CDF Collaboration), *Observation of Exclusive Electron-Positron Production in Hadron-Hadron Collisions*, Phys. Rev. Lett. 98 (2007) 112001, [arXiv:hep-ex/0611040].

[23] T. Aaltonen, et al., (CDF Collaboration), *Search for Exclusive Z-Boson Production and Observation of High-Mass $p\bar{p} \to p\gamma\gamma\bar{p} \to p\ell^+\ell^-\bar{p}$ Events in $p\bar{p}$ Collisions at $\sqrt{s} = 1.96$ TeV*, Phys. Rev. Lett. 102 (2009) 222002, [arXiv:0902.2816].

[24] T. Aaltonen, et al., (CDF Collaboration), *Search for Exclusive $\gamma\gamma$ Production in Hadron-Hadron Collisions*, Phys. Rev. Lett. 99 (2007) 242002, [arXiv:0707.2374];

Observation of Exclusive $\gamma\gamma$ Production in $p\bar{p}$ Collisions at $\sqrt{s} = 1.96$ TeV, Phys.Rev.Lett. 108 (2012) 081801, [arXiv:1112.0858].

[25] T. Aaltonen, et al., (CDF Collaboration), *Observation of exclusive dijet production at the Fermilab Tevatron $\bar{p}p$ collider*, Phys. Rev. D. 77 (2008) 052004, [arXiv:0712.0604].

[26] T. Aaltonen, et al., (CDF Collaboration), *Observation of Exclusive Charmonium Production and $\gamma\gamma \to \mu^+\mu^-$ in $p\bar{p}$ Collisions at $\sqrt{s} = 1.96$ TeV*, Phys. Rev. Lett. 102 (2009) 242001, [arXiv:0902.1271].

[27] M. Tasevsky, *Diffractive physics program in ATLAS experiment*, Nucl. Phys. Proc. Suppl. 179-180 (2008) 187-195; *Measuring Central Exclusive Processes at LHC*, [arXiv:0910.5205].

[28] C. Royon, (RP220 Collaboration), *Project to install roman pot detectors at 220 m in ATLAS*, [arXiv:0706.1796]; M.G. Albrow, et al., *FP420: An R&D proposal to investigate the feasibility of installing proton tagging detectors in the 420-m region at LHC*, CERN-LHCC-2005-025 (2005); B.E. Cox, (FP420 R and D Collaboration), *The FP420 R&D Project at the LHC*, [arXiv:hep-ph/0609209].

[29] C. Royon, *The ATLAS Forward Physics Project*, [arXiv:1302.0623].

[30] R. Staszewski, (ATLAS Collaboration), *The AFP Project*, Acta Physica Polonica B vol. 42 (2011) 1615, [arXiv:1104.1858].

[31] CMS Collaboration, *Search for new physics in monojet events in pp collisions at $\sqrt{s}$ = 8 TeV*, CMS-PAS-EXO-12-048.

[32] ATLAS Collaboration, *Search for New Phenomena in Monojet plus Missing Transverse Momentum Final States using $10fb^{-1}$ of pp Collisions at $\sqrt{s}$ = 8 TeV with the ATLAS detector at the LHC*, ATLAS-CONF-2012-147.

[33] V. M. Budnev, I. F. Ginzburg, G. V. Meledin, V. G. Serbo, *The two-photon particle production mechanism. Physical problems. Applications. Equivalent photon approx-*

imation, Phys. Rep. 15 (1975) 181; G. Baur, K. Hencken, D. Trautmann, S. Sadowsky and Y. Kharlov, *Coherent $\gamma\gamma$ and γA interactions in very peripheral collisions at relativistic ion colliders*, Phys. Rep. 364 (2002) 359, [arXiv:hep-ph/0112211]; K. Piotrzkowski, *Tagging two-photon production at the CERN Large Hadron Collider*, Phys. Rev. D 63 (2001) 071502, [hep-ex/0009065].

[34] J. de Favereau de Jeneret, V. Lemaitre, Y. Liu, S. Ovyn, T. Pierzchala, K. Piotrzkowski, X. Rouby, N. Schul, M. Vander Donckt, *High energy photon interactions at the LHC*, [arXiv:0908.2020].

[35] S. Ovyn, *Associated W and Higgs boson photoproduction and other electroweak photon induced processes at the LHC*, Nucl. Phys. Proc. Suppl. 179-180 (2008) 269-276, [arXiv:0806.1157].

[36] S. Ovyn, J. de Favereau de Jeneret, *High energy single top photoproduction at the LHC*, [arXiv:0806.4841].

[37] J. de Favereau de Jeneret, S. Ovyn, *Single top quark photoproduction at the LHC*, Nucl. Phys. Proc. Suppl. 179-180 (2008) 277-284, [arXiv:0806.4886].

[38] N. Schul, K. Piotrzkowski, *Detection of two-photon exclusive production of supersymmetric pairs at the LHC*, Nucl. Phys. Proc. Suppl. 179-180 (2008) 289-297, [arXiv:0806.1097]; K. Piotrzkowski, N. Schul, *Two-photon exclusive production of supersymmetric pairs at the LHC*, AIP Conf.Proc. 1200 (2010) 434-437, [arXiv:0910.0202].

[39] S. Heinemeyer, V. A. Khoze, M. G. Ryskin, W. J. Stirling, M. Tasevsky, G. Weiglein, *Studying the MSSM Higgs sector by forward proton tagging at the LHC*, Eur. Phys. J. C 53 (2008) 231-256, [arXiv:0708.3052]; *Central Exclusive Diffractive MSSM Higgs-Boson Production at the LHC*, J. Phys. Conf. Ser. 110 (2008) 072016, [arXiv:0801.1974]; S. Heinemeyer, V.A. Khoze, M.G. Ryskin, M. Tasevsky, G. Weiglein, *BSM Higgs Physics in the Exclusive Forward Proton Mode at the LHC*, Eur.

Phys. J. C 71 (2011) 1649, [arXiv:1012.5007]; Marek Tasevsky, *Exclusive MSSM Higgs production at the LHC after Run I*, Eur. Phys. J. C 73 (2013) 2672, [arXiv:1309.7772].

[40] S. Atag, S.C. Inan, I. Sahin, *Extra dimensions in photon-induced two lepton final states at the CERN-LHC*, Phys. Rev. D 80 (2009) 075009, [arXiv:0904.2687].

[41] S. Atag, S.C. Inan, I. Sahin, *Extra dimensions in $\gamma\gamma \to \gamma\gamma$ process at the CERN-LHC*, JHEP 09 (2010) 042, [arXiv:1005.4792].

[42] Hao Sun, *Large Extra Dimension effects through Light-by-Light Scattering at the CERN LHC*, Eur. Phys. J. C 74 (2014) 2977, [arXiv:1406.3897].

[43] I. Sahin, A.A. Billur, S.C. Inan, B. Sahin, M. Koksal, P. Tektas, E. Alici, R. Yildirim, *Probe of extra dimensions in $\gamma q \to \gamma q$ at the LHC* , Phys. Rev. D 88 (2013) 095016, [arXiv:1304.5737].

[44] I. Sahin, S. C. Inan, *Probe of unparticles at the LHC in exclusive two lepton and two photon production via photon-photon fusion*, JHEP 0909 (2009) 069, [arXiv:0907.3290].

[45] Hao Sun, Chong-Xing Yue, *Precise photoproduction of the charged top-pions at the LHC with forward detector acceptances*, Eur. Phys. J. C 74 (2014) 2823, [arXiv:1401.0250].

[46] T. Pierzcha la, K. Piotrzkowski, *Sensitivity to anomalous quartic gauge couplings in photon-photon interactions at the LHC*, Nucl.Phys.Proc.Suppl. 179-180 (2008) 257-264, [arXiv:0807.1121].

[47] O. Kepka, C. Royon, *Anomalous $WW\gamma$ coupling in photon-induced processes using forward detectors at the CERN LHC*, Phys. Rev. D 78 (2008) 073005, [arXiv:0808.0322].

[48] C. Royon, E. Chapon, O. Kepka, *Anomalous trilinear and quartic $WW\gamma$, $WW\gamma\gamma$, $ZZ\gamma$ and $ZZ\gamma\gamma$ couplings in photon induced processes at the LHC*, PoS EPS-HEP2009 (2009) 380, [arXiv:0909.5237].

[49] E. Chapon, C. Royon, O. Kepka, *Anomalous quartic $WW\gamma\gamma$, $ZZ\gamma\gamma$, and trilinear $WW\gamma$ couplings in two-photon processes at high luminosity at the LHC*, Phys. Rev. D 81 (2010) 074003, [arXiv:0912.5161].

[50] I. Sahin, A. A. Billur, *Anomalous $WW\gamma$ couplings in $\gamma-$proton collision at the LHC*, Phys. Rev. D 83 (2011) 035011, [arXiv:1101.4998].

[51] Rick S. Gupta, *Probing quartic neutral gauge boson couplings using diffractive photon fusion at the LHC*, Phys. Rev. D 85 (2012) 014006, [arXiv:1111.3354].

[52] I. Sahin, B. Sahin, *Anomalous quartic $ZZ\gamma\gamma$ couplings in γ proton collision at the LHC*, Phys. Rev. D 86 (2012) 115001, [arXiv:1211.3100].

[53] A. Senol, *$ZZ\gamma$ and $Z\gamma\gamma$ anomalous couplings in γp collision at the LHC*, Phys. Rev. D 87 (2013) 073003, [arXiv:1301.6914].

[54] A. Senol, *Anomalous quartic $WW\gamma\gamma$ and $ZZ\gamma\gamma$ couplings in γp collision at the LHC*, [arXiv:1311.1370].

[55] S. Fichet, G. von Gersdorff, O. Kepka, B. Lenzi, C. Royon, M. Saimpert, *Probing new physics in diphoton production with proton tagging at the Large Hadron Collider*, [arXiv:1312.5153].

[56] I. Sahin, M. Koksal, *Search for electromagnetic properties of the neutrinos at the LHC*, JHEP 1103 (2011) 100, [arXiv:1010.3434].

[57] S. Atag, A.A. Billur, *Possibility of Determining τ Lepton Electromagnetic Moments in $\gamma\gamma \to \tau^+\tau^-$ Process at the CERN-LHC*, JHEP 1011 (2010) 060, [arXiv:1005.2841].

[58] I. Sahin, *Electromagnetic properties of the neutrinos in γ-proton collision at the LHC*, Phys. Rev. D 85 (2012) 033002, [arXiv:1201.4364].

[59] M.Köksal, S. C. Inan, *Anomalous $tq\gamma$ couplings in γp collision at the LHC*, [arXiv:1305.7096].

[60] Hao Sun, *Probe Anomalous $tq\gamma$ couplings through Single Top Photoproduction at the LHC*, Nucl. Phys. B 886 (2014) 691-711, [arXiv:1402.1817].

[61] B. Sahin, A. A. Billur, *Anomalous Wtb couplings in γ-proton collision at the LHC*, Phys. Rev. D 86 (2012) 074026, [arXiv:1210.3235].

[62] M. Chaichian, P. Hoyer, K. Huitu, V.A. Khoze, A.D. Pilkington, *Searching for the triplet Higgs sector via central exclusive production at the LHC*, JHEP 0905 (2009) 011, [arXiv:0901.3746].

[63] M. Beltran, D. Hooper, E.W. Kolb and Z.C. Krusberg, *Deducing the nature of dark matter from direct and indirect detection experiments in the absence of collider signatures of new physics*, Phys. Rev. D 80 (2009) 043509, [arXiv:0808.3384]; Hao Zhang, Qing-Hong Cao, Chuan-Ren Chen, Chong Sheng Li, *Effective Dark Matter Model: Relic density, CDMS II, Fermi LAT and LHC*, JHEP 1108 (2011) 018, [arXiv:0912.4511]; J. Goodman, M. Ibe, A. Rajaraman, W. Shepherd, T.M.P. Tait and H.-B. Yu, *Constraints on Light Majorana Dark Matter from Colliders*, Phys. Lett. B 695 (2011) 185, [arXiv:1005.1286].

[64] J. Beringer et al., (Particle Data Group), *Review of Particle Physics (RPP)*, Phys. Rev. D 86 (2012) 010001.

[65] T. Hahn, *Generating Feynman diagrams and amplitudes with FeynArts 3*, Comput. Phys. Commun. 140 (2001) 418-431, [arXiv:hep-ph/0012260].

[66] T. Hahn, *Automatic Loop Calculations with FeynArts, FormCalc, and LoopTools*, Nucl. Phys. Proc. Suppl. 89 (2000) 231-236, [arXiv:hep-ph/0005029]. S. Agrawal, T. Hahn, E. Mirabella, *FormCalc 7*, J. Phys. Conf. Ser. 368 (2012) 012054, [arXiv:1112.0124].

[67] T. Hahn, M. Perez-Victoria, *Automatized one loop calculations in four-dimensions and D-dimensions*, Comput. Phys. Commun. 118 (1999) 153-165, [arXiv:hep-ph/9807565].

[68] Marco Guzzi, Pavel Nadolsky, Edmond Berger, Hung-Liang Lai, Fredrick Olness, C.-P. Yuan, *CT10 parton distributions and other developments in the global QCD analysis*, SMU-HEP-10-11, [arXiv:1101.0561].

[69] S. Kawabata, *A new version of the multi-dimensional integration and event generation package BASES/SPRING*, Comp. Phys. Commun 88 (1995) 309-326; F. Yuasa, D. Perret-Gallix, S. Kawabata, T. Ishikawa, *Pvm-grace*, Nucl. Instrum. Meth. A389 (1997) 77-80.

[70] V. A. Khoze, A. D. Martin and M. G. Ryskin, *Prospects for New Physics observations in diffractive processes at the LHC and Tevatron*, Eur. Phys. J. C 23 (2002) 311, [arXiv:hep-ph/0111078].

[71] Ingelman and Schlein, Phys. Lett. B152 (1985) 256.

[72] A. Aktas, et al., (H1 Collaboration), *Measurement and QCD analysis of the diffractive deep-inelastic scattering cross-section at HERA*, Eur. Phys. J. C 48 (2006) 715, [hep-ex/0606004].

[73] A. Aktas, et al., (H1 Collaboration), *Dijet Cross Sections and Parton Densities in Diffractive DIS at HERA*, JHEP 0710 (2007) 042, [arXiv:0708.3217].

[74] G. L. Bayatian, et al., (CMS Collaboration), J. Phys. G 34 (2007) 995.

[75] P. J. Fox, R. Harnik, J. Kopp and Y. Tsai, *LEP Shines Light on Dark Matter*, Phys. Rev. D 84 (2011) 014028, [arXiv:1103.0240].

[76] Yoonseok John Chae, Maxim Perelstein, *Dark Matter Search at a Linear Collider: Effective Operator Approach*, JHEP 1305 (2013) 138, [arXiv:1211.4008].

[77] Maria Beltran, Dan Hooper, Edward W. Kolb, Zosia A. C. Krusberg, Tim M. P. Tait, *Maverick dark matter at colliders*, JHEP 1009 (2010) 037, [arXiv:1002.4137].

[78] Ian M. Shoemaker, Luca Vecchi, *Unitarity and Monojet Bounds on Models for DAMA, CoGeNT, and CRESST-II*, Phys.Rev. D86 (2012) 015023, [arXiv:1112.5457].

[79] A. Cisek, W. Schafer, A. Szczurek, *Production of Z^0 bosons with rapidity gaps: Exclusive photoproduction in γp and pp collisions and inclusive double diffractive $Z^{0\prime}s$*, Phys. Rev. D 80 (2009) 074013, [arXiv:0906.1739].